Development 130, 3841-3850

doi:10.1242/dev.00564

FRIZZY PANICLE is required to prevent the formation of axillary meristems and to establish floral meristem identity in rice spikelets

Mai Komatsu[1,2], Atsushi Chujo[1], Yasuo Nagato[1], Ko Shimamoto[2] and Junko Kyozuka[1,3,*]

[1]Graduate School of Agricultural and Life Sciences, University of Tokyo, Tokyo 113-8657, Japan
[2]Graduate School of Biological Sciences, Nara Institute of Science and Technology, Ikoma, Nara 630-0101, Japan
[3]CREST, Japan Science and Technology Corporation, Tokyo 101-0062, Japan
*Author for correspondence (e-mail: akyozuka@mail.ecc.u-tokyo.ac.jp)

Accepted 24 April 2003

SUMMARY

Inflorescences of grass species have a distinct morphology in which florets are grouped in compact branches called spikelets. Although many studies have shown that the molecular and genetic mechanisms that control floret organ formation are conserved between monocots and dicots, little is known about the genetic pathway leading to spikelet formation. In the *frizzy panicle* (*fzp*) mutant of rice, the formation of florets is replaced by sequential rounds of branching. Detailed analyses revealed that several rudimentary glumes are formed in each ectopic branch, indicating that meristems acquire spikelet identity. However, instead of proceeding to floret formation, axillary meristems are formed in the axils of rudimentary glumes and they either arrest or develop into branches of higher order. The *fzp* mutant phenotype suggests that *FZP* is required to prevent the formation of axillary meristems within the spikelet meristem and permit the subsequent establishment of floral meristem identity. The *FZP* gene was isolated by transposon tagging. *FZP* encodes an ERF transcription factor and is the rice ortholog of the maize *BD1* gene. Consistent with observations from phenotypic analyses, *FZP* expression was found to be restricted to the time of rudimentary glumes differentiation in a half-ring domain at the base of which the rudimentary glume primordium emerged.

Key words: Rice inflorescence, Meristem identity, ERF transcription factor

INTRODUCTION

Plants continue organogenesis throughout their lifetime by initiating a multitude of lateral growth axes from the periphery of meristems, the source of plant stem cells. These lateral growth axes can form organs such as leaves and lateral shoots. In the reproductive phase, the shoot meristem acquires inflorescence meristem identity and produces secondary meristems that can either give rise to flowers, if taking floral meristem identity, or produce further lateral branches, if taking branch meristem identity. The overall pattern of branching and flower formation, which results from the pattern of changes in meristem identity, determines the architecture of the inflorescence (Coen and Nugent, 1994). Grass inflorescences show a third and unique type of secondary meristem, the spikelet meristem, from which groups of small flowers called florets emerge. The formation of the spikelet makes the study of the genetic pathways leading to flowering in grasses particularly interesting.

The spikelet is the ultimate unit of the grass inflorescence and comprises a series of modified leaves called bracts and florets. Among the bracts, the one subtending the floral meristem is specifically called a lemma. The floral meristem produces the floral organs – palea, lodicules, stamens and carpel – that together with the subtending lemma are termed as a floret. The number of florets per spikelet varies between grass species and in the case of rice, a single floret is subtended by two pairs of bracts called empty glumes and rudimentary glumes (Fig. 1E, Fig. 2C,D). Usually, the structure containing the floret and the empty glumes, but not the rudimentary glumes, is considered to be a rice spikelet (Hoshikawa, 1989; Bell, 1991; Takeoka et al., 1993). Despite the distinct terminology, molecular analyses based on the well-established ABC model of floral organ identity have proved that lodicules are the counterparts of dicot petals and indicate that the palea and possibly the lemma are equivalents to sepals (Kang et al., 1998; Ambrose et al., 2000; Kyozuka et al., 2000; Goto et al., 2001). However, although grass florets are similar to dicot flowers, the nature of the spikelet remains unclear.

The fact that the formation of a spikelet requires a meristem fate distinct from those observed in dicot species implies that different molecular mechanisms may control spikelet initiation. One important question is whether a conserved regulatory pathway operates or whether novel genes are recruited for floral determination in grasses. In addition, how the identities of spikelet and floral meristems are differentially controlled remains to be answered. Although several mutations that affect the change from branch to spikelet and spikelet to floret meristem have been reported, to date, only a few genes have been isolated (reviewed by McSteen et al., 2000). For

example, in the *branched silkless1* (*bd1*) mutant, indeterminate branches are formed in the place of spikelets in the ear and extra spikelets are formed in the tassel (Colombo et al., 1998). Recently, the *BD1* gene was reported to be a member of the ERF family of transcription factors, and it was proposed that signaling pathways involving *BD1* regulate meristem identity from the lateral domains of spikelet meristems (Chuck et al., 2002). It is expected that the identification of more genes will unveil the genetic framework that rules the development of inflorescences in grasses.

With the completion of the rice genome sequence (http://rgp.dna.affrc.go.jp/) and the availability of an abundant collection of mutants affecting reproductive development (Kinoshita and Takahashi, 1991; Murai and Iizawa, 1994; Kyozuka, 1999), the forward genetics approach in rice is expected to be a powerful strategy to identify genes involved in grass inflorescence development. Among rice inflorescence mutants, *frizzy panicle* (*fzp*) is of particular interest (Fig. 2E-L). Although inflorescence mutations tend to influence more than one type of meristem (McSteen et al., 2000; Battey and Tooke, 2002), *fzp* shows defects only in spikelet development. In the inflorescence of the *fzp* mutant, primary branch meristems develop normally but secondary branch meristems are produced in place of all spikelets, resulting in the formation of an abnormal inflorescence composed of a mass of branch shoots (Komatsu et al., 2001). The reversion of spikelet meristems to branch meristems is very similar to the phenotype observed in the ear of maize *bd1* mutants and indicates that *FZP* is also required to specify spikelet meristem identity. Here we describe a more detailed analysis of the *fzp* phenotype and the isolation of the *FZP* gene, which encodes an ERF transcription factor and is the rice ortholog of the maize *BD1* gene. Our data suggest that *FZP* prevents the outgrowth of the axillary meristem within the rudimentary glume and maintains the transition from spikelet to floral meristem identity.

MATERIALS AND METHODS

Plant materials

In addition to the previously described *fzp* and *fzp2* mutants (Komatsu et al., 2001), six more mutants showing a similar phenotype were identified. For complementation tests, plants that were heterozygous for the *fzp*-like mutation were crossed. Segregation of normal and mutant inflorescences in a 3:1 ratio in the F_1 population demonstrated that they were alleles (data not shown). Therefore, *fzp* was re-designated as *fzp-1*, *fzp2* as *fzp-2* and the new three alleles were called *fzp-3*, *fzp-4* and *fzp-5*. The other three mutants were designated *fzp-FM44*, *fzp-KH1* and *fzp-KH56*.

The *fzp-4* and *fzp-5* alleles were obtained from a pool of approximately 9000 selfed lines carrying the maize *Ac* transposon as previously described (Enoki et al., 1999); *fzp-3*, *fzp-KH1* and *fzp-KH56* were obtained by EMS-induced mutagenesis and *fzp-FM44* was obtained by spontaneous mutation. All alleles and *fzp*-like mutants were of the *japonica* variety of *Oryza sativa* L. and the background cultivars were: M201 for *fzp-1*; Shiokari for *fzp-2*; Hanaetizen for *fzp-3*; Toride for *fzp-4* and *fzp-5*; Koshihikari for *fzp-KH1* and *fzp-KH56*, and unknown for *fzp-FM44* (Table 1). The wild-type cultivar used was Toride. Plants were grown at 27°C in a greenhouse with 16 hours light and 8 hours darkness.

SEM analyses

Young inflorescences of wild-type, *fzp-2* and *fzp-3* seedlings were dissected and fixed overnight at 4°C in a 2.5% formaldehyde solution. After dehydration through an ethanol series of 50-100%, critical point drying, mounting and carbon coating, specimens were examined in a Hitachi S-4700 scanning electron microscope (Hitachi High-Technologies Corp., Tokyo, Japan).

Mapping

Rough mapping of the *FZP* locus was performed using cleaved amplified polymorphic sequence (CAPS) markers, which were constructed on the basis of the sequence information provided by the National Institute of Agrobiological Sciences (NIAS, Japan). dCAPS markers, constructed according to Michaels and Amasino (Michaels and Amasino, 1998), were utilized for the fine mapping of the *FZP* locus. In the F_2 generation of our mapping population of *fzp-3 japonica* cv. Hanaetizen crossed to wild-type *indica* cv. Kasalath, we detected linkage of the *fzp* mutation to the markers RA1789 and 3817R with 5 mutant plants each out of 178. Recombinants were then genotyped with dCAPS markers in the interval between 4016R and 3997R. This delimited the *FZP* locus to a region of 119 kb on chromosome 7 covered by the overlapping PAC clones AP004300 and AP004570. Further mapping was not continued after the identification of the transposon-tagged allele.

Southern blot analysis and cloning of the *FZP* gene

DNA (5 μg) extracted from *fzp-4* seedlings were digested with *Eco*RI, separated by electrophoresis and blotted as described previously (Enoki et al., 1999). The C-terminal half of the maize *Ac* element was amplified by polymerase chain reaction (PCR) using primers 5′-TCCAACAATGATTGGTGATCTCG-3′ and 5′-CATATTTAACTT-GCGGGACGGAAAC-3′, and the resultant product was used as probe. Inverse PCR (Trigrlia et al., 1988) of *Eco*RI-digested DNA was applied to isolate the sequences flanking the *Ac* elements using primers 5′-CGGTTATACGATAACGGTCGGTAC-3′ and 5′-TGAAG-TGTGCTAGTGAATGTGACTTG-3′ for the N-terminal flanks and 5′-TAAGGCATCCCTCAACATCAAATAG-3′ and 5′-GATTACCG-TATTATCCCGTTCG-3′ for the C-terminal flanks. The GenBank accession number of the *FZP* cDNA is AB103120.

Transient expression

The GAL4-responsive reporter construct (GAL4-LUC) contained five copies of the GAL4 binding site in tandem and a minimal TATA region of the CaMV 35S promoter, the firefly gene for luciferase (LUC) and a nopaline synthase (NOS) terminator (Ohta et al., 2000). The effector constructs were driven by the CaMV 35S promoter and contained a GAL4 DNA-binding domain (GAL4DB) or the coding region of *FZP* fused to the latter (GAL4DB-FZP). A translational enhancer sequence from the tobacco mosaic virus (Ω) was placed upstream of the translation initiation sites. Transient assays in *Arabidopsis* leaves were performed by using the particle gun bombardment method as described previously (Fujimoto et al., 2000; Ohta et al., 2001). Luciferase assays were performed with the dual-luciferase reporter assay system. To normalize values after each transfection, the *Renilla* luciferase gene under the control of the CaMV 35S promoter was used as an internal control (Ohta et al., 2000). The values cited are averages, with standard deviations, of results obtained from 3 independent experiments. Normalized luciferase activity recorded after transfection with the GAL4-LUC plasmid alone was set arbitrarily at 1.

In situ hybridization

The N-terminal and the C-terminal halves of the *FZP* coding region excluding the ERF domain were amplified by PCR using three sets of primers as follows: 5′-GTCATGAACACTCGAGGC-3′ and 5′-CTCCCTGGCTCCTGCGC-3′, 5′-CACATTGGCTCGTACGGTC-3′ and 5′-GAGAAGAGGAAGTCGTGG-3′, 5′-CCACGACTTCCTC-TTCTCCG-3′ and 5′-CCGGCGACCATCTGC-3′. PCR products were cloned into p-GEM-T vectors (Promega Corporation, Madison,

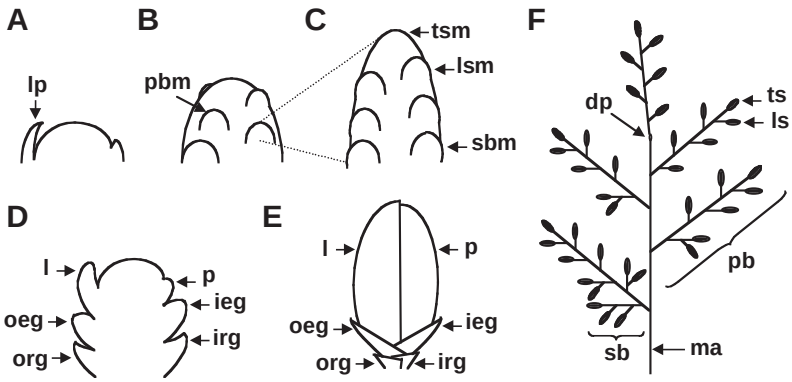

Fig. 1. Scheme depicting the development of the shoot apical meristem (SAM) of rice. (A) Vegetative meristem. Leaf primordia emerge from the SAM in an alternate phyllotaxis. (B) Reproductive meristem at the stage of primary branch meristem (PBM) formation. PBMs emerge spirally from the SAM at 144° from the previous one. (C) PBM at the spikelet and secondary branch meristem (SBM) formation stage. Meristems emerge from the primary branches in two alternate rows. Upper meristems acquire lateral SM identity whereas lower meristems form SBMs. The PBM itself acquire terminal SM identity. (D) SM at floret formation stage. Rudimentary glumes, empty glumes, lemma and palea primordia emerge alternately from the SM. (E) Schematic representation of a mature rice spikelet. Floral organs (not represented) are enclosed by the lemma and palea. (F) Schematic representation of a mature rice inflorescence. lp, leaf primordium; pbm, primary branch meristem; tsm, terminal spikelet meristem; lsm, lateral spikelet meristem; sbm, spikelet branch meristem; org, outer rudimentary glume; irg, inner rudimentary glume; oeg, outer empty glume; ieg, inner empty glume; l, lemma; p, palea; ma, main axis; pb, primary branch; sb, secondary branch; ts, terminal spikelet; ls, lateral spikelet; dp, degenerate point.

USA), linearized and used as templates for making digoxigenin-labeled sense and anti-sense RNA probes. The three probes were used simultaneously for hybridization. Tissue fixation and in situ hybridization procedures were performed as described previously (Kyozuka et al., 2000), except that sections were washed in SSC solution and two washes of 20 minutes were performed after RNase treatment.

RESULTS

Spikelets are replaced by branches in mutants carrying severe *fzp* alleles

The development of rice inflorescences is schematized in Fig. 1 (see also Hoshikawa, 1989; Takeoka et al., 1992; Takeoka et al., 1993). In wild-type plants of rice, the shoot apical meristem (SAM) initiates leaf primordia alternately with a divergence angle of 180° (Fig. 1A). In the transition to reproductive development, the SAM acquires inflorescence meristem (IM) identity and primary branch meristems (PBMs) initiate in a spiral phyllotaxy (Fig. 1B). The phyllotaxy changes one more time and lateral spikelet meristems (SMs) and secondary branch meristems (SBMs) are initiated alternately from the primary branches forming two rows (Fig. 1C). Rudimentary glumes, empty glumes, lemma and palea primordia are also initiated in the SM in an alternate phyllotaxy (Fig. 1D,E). The IM degenerates after the production of the primary branch primordia, whereas the PBMs and SBMs are converted to terminal spikelets (Fig. 1F). PBMs, SBMs and SMs are initiated as axillary meristems in the axils of bract primordia, but as they do not develop further only bracts are visible in the mature inflorescence (arrow in Fig. 2D). The mature wild-type inflorescence is composed of a main axis, primary branches, short secondary branches and terminal and lateral spikelets (Fig. 1F, Fig. 2A-D).

We have previously described the phenotype of *fzp2*, a rice inflorescence mutant that resembled the *fzp* mutant reported by Mackill et al. (Mackill et al., 1991; Komatsu et al., 2001). Complementation tests showed that *fzp2* is allelic to *fzp* (Materials and Methods) and, therefore, we redesignated the later as *fzp-1* and the former as *fzp-2* (Table 1). Further analyses of the morphology of *fzp-2* inflorescences were performed. In *fzp-2* plants, the development of the SAM did not differ from wild-type plants until primary branches were formed (Komatsu et al., 2001). However, all meristems on a primary branch initiated secondary branches without forming spikelets (Fig. 2E,F). These secondary branches were composed of several bract-like structures arranged in an alternate phyllotaxy (inset in Fig. 2F). Tertiary branches were formed in the axils of the bract-like structures in the upper part of the secondary branch, and they were also composed of bract-like structures with apical higher order branches (Fig. 2G,H, Fig. 3A). SEM analyses of *fzp-2* tertiary branches revealed that higher order branch meristems were formed at 90° to the previous order branches (Fig. 3A,C). Considering that spikelet meristems and spikelet organs are formed in an alternate phyllotaxy in wild-type inflorescences, the phyllotaxy of bract-like structures in *fzp-2* indicates that the defect on the mutant occurs after the acquisition of spikelet meristem identity, as we have observed previously (Komatsu et al., 2001).

Table 1. *fzp* alleles used in this study

Alleles (former name)	Background cultivar	Phenotype	Origin
fzp-1 (fzp)	M-201	Severe	EMS mutagenesis
fzp-2 (fzp2)	Shiokari	Severe	γ-ray mutagenesis
fzp-3	Hanaetizen	Weak	EMS mutagenesis
fzp-4	Toride	Severe	*Ac* transgenic pool
fzp-5	Toride	Severe	*Ac* transgenic pool
fzp-6 (fzp-FM44)	Unknown	Temperature sensitive	Spontaneous
fzp-7 (fzp-KH56)	Koshihikari	Severe	EMS mutagenesis
fzp-8 (fzp-KH1)	Koshihikari	Severe	EMS mutagenesis

Spikelets are formed at the apices of ectopic branches in plants with weak *fzp* alleles

In addition to *fzp-1* and *fzp-2*, another three alleles, designated *fzp-3* to *fzp-5* and three more mutants, designated *fzp-FM44*, *fzp-KH1* and *fzp-KH56*, were obtained (Materials and Methods, Table 1). While the phenotypes of *fzp-4*, *fzp-KH1* and *fzp-KH56* were similar to those of *fzp-1* and *fzp-2*, *fzp-3* and *fzp-FM44* showed weaker phenotypes. In *fzp-3* mutants, primary branches initiated secondary branches that exhibited bract-like structures, as occurred with the severe alleles, but

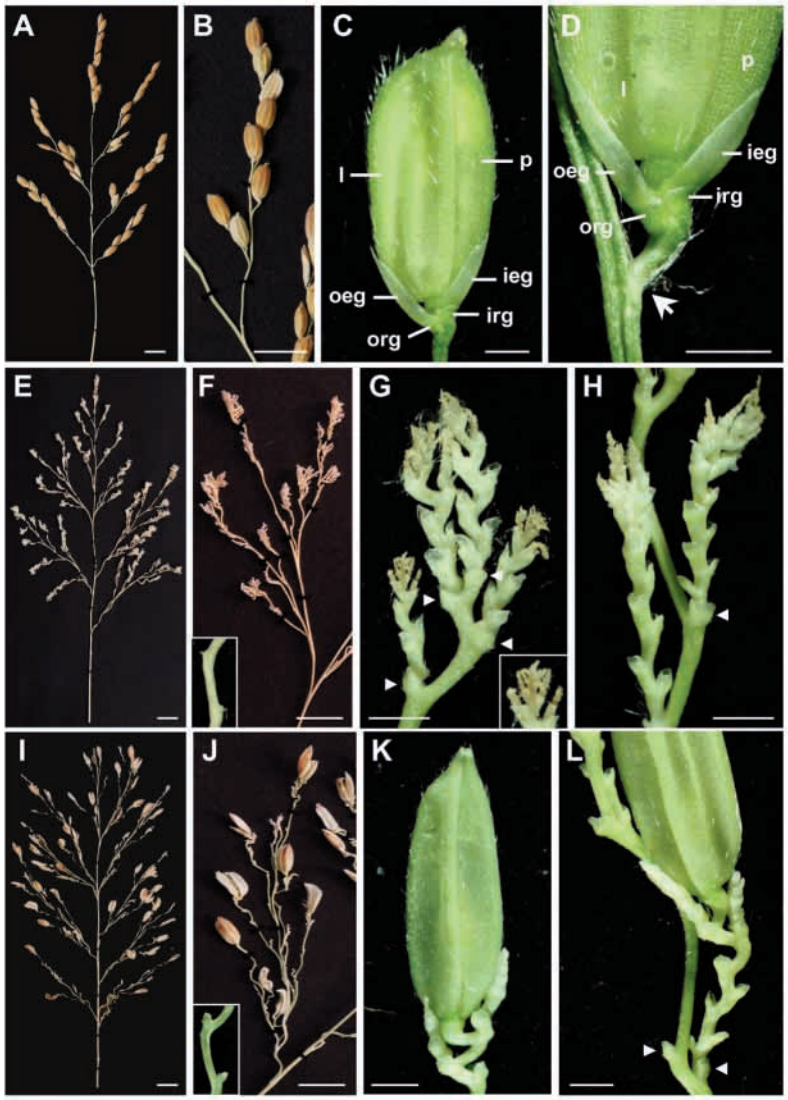

Fig. 2. Morphology of wild-type, severe and weak *fzp* inflorescences, spikelets and ectopic branches. (A-D) Wild type. (E-H) *fzp-2*. (I-L) *fzp-3*. The wild-type inflorescence (A) is composed of primary branches (B) and secondary branches that have terminal (C) and lateral (D) spikelets. Bracts are not observed at the junction between the spikelet pedicel and the growth axis (D arrow). (E,F) Spikelets are replaced by branches in the severe *fzp-2* allele, but defective and normal spikelets can be formed at the apices of ectopic branches of the weak *fzp-3* allele (I,J). *fzp-2* and *fzp-3* secondary branches are composed of alternate bract-like structures (F,J, insets). Tertiary branches develop at the axils of the bract-like structures (G,H,L arrowheads) in the apical part of a secondary branch and they are also composed of bract-like structures that form higher order branches at their axils (G inset). (G) The apices of a *fzp-2* secondary branch is terminated with a tertiary branch. (K,L) *fzp-3* tertiary branches are terminated with a spikelet. org, outer rudimentary glume; irg, inner rudimentary glume; oeg, outer empty glume; ieg, inner empty glume; l, lemma; p, palea. Scale bars: 1 cm (A,B,E,F,I,J); 1 mm (C,D,G,H,K,L).

could form fertile or defective spikelets at their tips (Fig. 2I,J). These spikelets were formed in the axils of the bract-like structures of tertiary branches, which also generated higher order branches (Fig. 2K,L). SEM analysis of *fzp-3* tertiary branches revealed that whereas defective and fertile spikelets were formed at the majority of branch tips, higher order lateral branches did not form spikelets (Fig. 3B,D,E). The phenotype of the *fzp-FM44* was temperature sensitive and it could be as severe as that of *fzp-2* under low temperatures, or normal, as in wild-type, with fertile terminal and lateral spikelets, when grown at optimal temperatures (data not shown).

Rudimentary glumes with axillary meristems are produced in *fzp* mutants

Every ectopic branch in the plants with weak and severe *fzp* alleles produced several bract-like structures that developed alternately from the main axis and appeared very similar to wild-type rudimentary glumes (compare Fig. 2C,D with G,H,L). Molecular markers for rudimentary glumes are not available at present. Therefore, in order to establish if the bract-like structures were actually rudimentary glumes, the cell types of these structures were examined more closely by SEM.

In wild-type spikelets whereas the empty glumes had flat cells of regular shape that rarely exhibited hairs resulting in an overall smooth appearance, the rudimentary glume cells had an irregular shape and had hairs that could be short or long resulting in a rugous appearance (Fig. 4A-D). The bract-like structures of the mutants showed a cell type very similar to the one observed for rudimentary glumes with irregular shape and a protruding hair (Fig. 4E,F), strongly indicating that the bract-like structures were actually

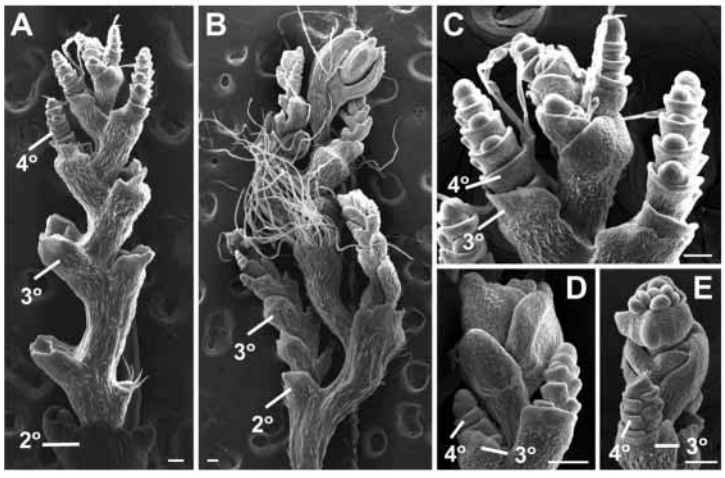

Fig. 3. SEM analysis of *fzp-2* and *fzp-3* ectopic branches. (A,C) *fzp-2*. (B,D,E) *fzp-3*. (A) Tertiary branch of *fzp-2*. Note that the direction of outgrowth of bract-like structures is at 90° to the previous branch. (B) Tertiary branches on a secondary branch of *fzp-3*. (C) The apex of a *fzp-2* tertiary branch terminates with the formation of quaternary branches. (D,E) The majority of *fzp-3* tertiary branches form defective spikelets at their tips. 2°, bract-like structure of secondary order branches; 3°, tertiary order; 4°, quaternary order. Scale bars: 100 μm.

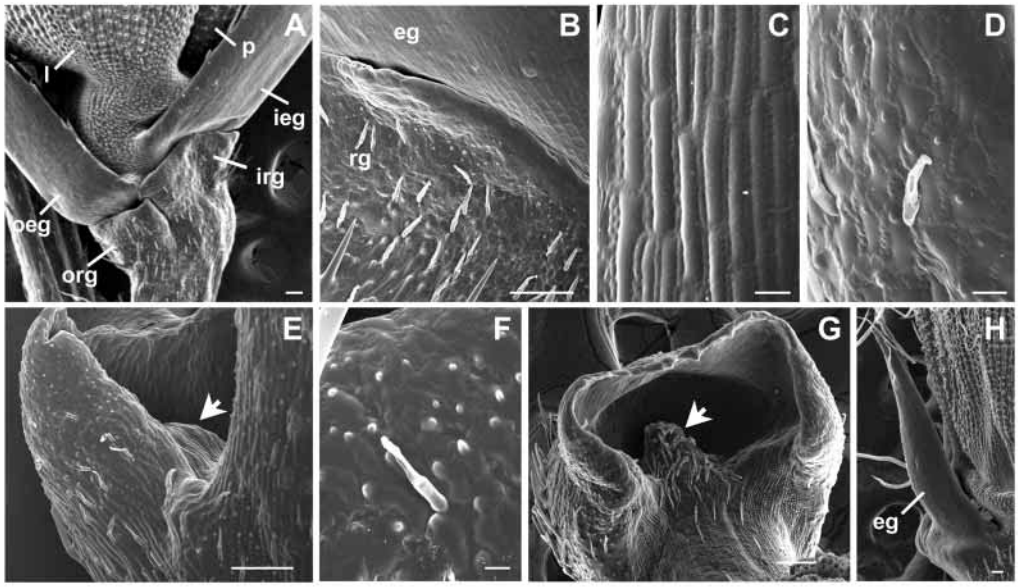

Fig. 4. SEM analysis of wild-type spikelet organs and *fzp-2* bract-like structures. (A) Junction between the organs of a wild-type spikelet. (B) Border between the rudimentary glume and the empty glume of a wild-type spikelet. (C) The cells of empty glumes have a regular shape and a flat surface that result in a smooth overall appearance. (D) The cells of rudimentary glumes have a irregular shape and hairs that can be short or long, resulting in a rugous appearance. (E) Bract-like structure of a *fzp-2* tertiary branch. An axillary meristem (arrow) is formed but its development is arrested. (F) The cells of bract-like structures of *fzp* mutants have irregular shape and hairs similar to the cells of wild-type rudimentary glumes. (G) Upper view of a bract-like structure and its degenerated axillary meristem (arrow) on the secondary branch of a *fzp-2* spikelet. (H) Empty glume of a *fzp-3* spikelet. org, outer rudimentary glume; irg, inner rudimentary glume; oeg, outer empty glume; ieg, inner empty glume; l, lemma; p, palea; eg, empty glume; rg, rudimentary glume. Scale bars: 100 μm (A,B,E,G,H); 10 μm (C,D,F).

rudimentary glumes. Although empty glumes were only rarely observed in spikelets of the weak *fzp-3* mutant, some had empty glume-like structures. SEM analyses revealed that their cell type was similar to that of wild-type empty glumes (Fig. 4G).

While higher order branches were observed only in the axils of ectopic rudimentary glumes localized at the upper part of an ectopic branch, SEM analyses revealed that lower rudimentary glumes also contained degenerated axillary meristems (Fig. 4E,H). We have previously determined that all meristems remained undifferentiated during the early development of *fzp* inflorescences (Komatsu et al., 2001). Therefore, the degeneration of these axillary meristems might occur during the maturation stage when internodes elongate. Why all axillary meristems do not develop into a branch remains unclear. Nevertheless, to our knowledge, axillary meristem formation from rudimentary glumes is not reported to occur in wild-type spikelets.

FZP is the rice ortholog of the maize *BD1* gene

A map-based approach was initially applied to clone the *FZP* gene (Materials and Methods). The *FZP* locus was delimited to a 119 kb interval on chromosome 7 covered by two overlapping PAC clones, AP004570 and AP004300 (Fig. 5A). At the same time, one line showing the severe *fzp* phenotype (*fzp-4*) was found in a population of transgenic rice plants carrying the maize *Ac* element (Fedoroff et al., 1983; Izawa et al., 1997). After detecting co-segregation of two tightly linked

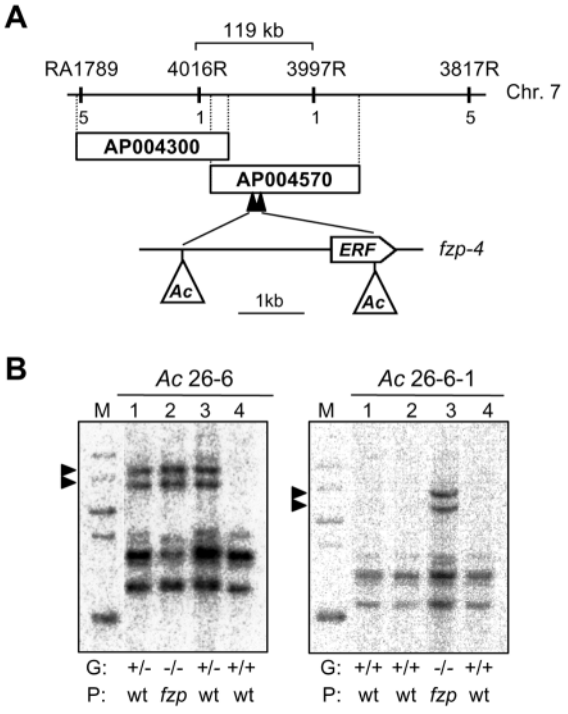

Fig. 5. Cloning of the *FZP* gene. (A) A map-based strategy was initially applied to clone the *FZP* gene but was discontinued with the identification of a transposon-tagged mutant. (Top) The markers flanking the *FZP* locus and the number of recombinants in a mapping population of 178 plants are indicated. *FZP* was delimited to a region of 119 kb covered by two PAC clones. (Bottom) The *fzp-4* allele showed two *Ac* transposon insertions in a region corresponding to the AP004570 PAC clone; the distal *Ac* element disrupted a putative ERF-like gene. (B) Co-segregation of two *Ac* elements with the *fzp* phenotype (arrowheads) in *fzp-4* seedlings. (Left) Southern hybridization of four seedlings of the parental *Ac* 26-6 line. (Right) Southern hybridization of four seedlings of the progeny of the *Ac* 26-6-1 seedling. The genotype (G) of the *fzp* locus disruption and phenotype (P) of each seedling are indicated below. +/–, heterozygous; –/–, homozygous mutant; +/+, homozygous wild type; wt, wild-type; *fzp*, *frizzy panicle*. M, marker: 3, 5, 6, 8, 10 kb from the bottom to the top.

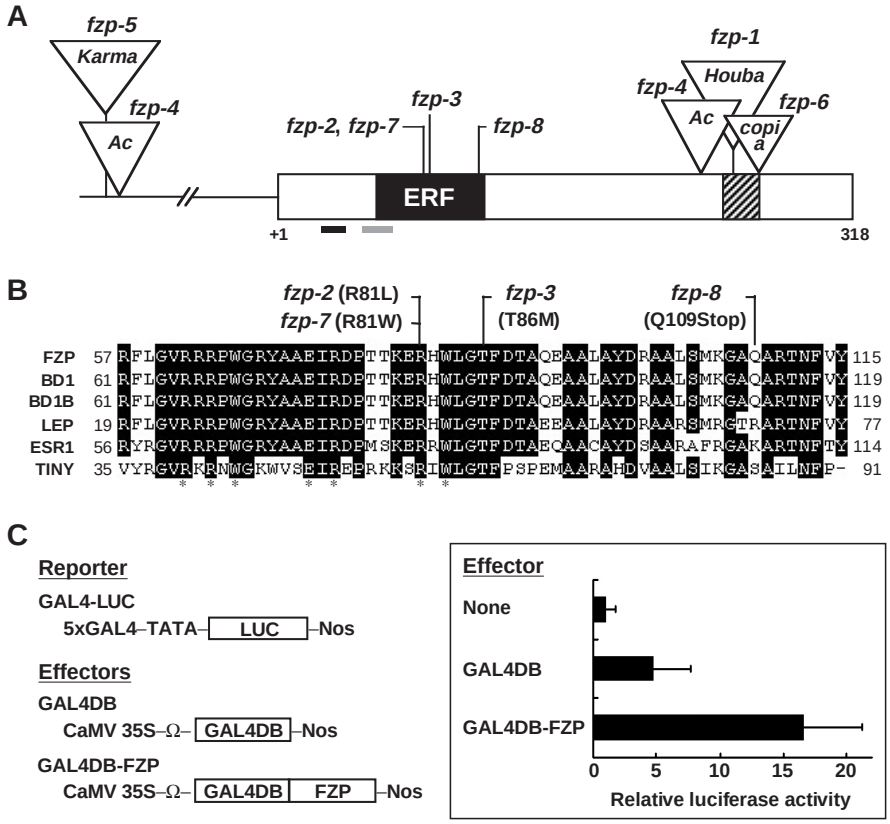

Fig. 6. Structure of the *FZP* gene and similarity to other ERF transcription factors. (A) Schematic representation of the *FZP* gene structure with mutant lesions. The ERF domain (black box) is localized at the N-terminal half whereas the acidic domain (hatched box) conserved in grass BD1-like proteins is closer to the C terminus. The position of the mutations in the *fzp* alleles are indicated above. The amino acid numbers are indicated below. The black line indicates the putative PEST sequence and the grey line indicates the bipartite nuclear localization signal. (B) Alignment of the amino acid sequences of the ERF domains of *FZP* and other members of the ERF family. Asterisks indicate amino acids that confer specific GCC-box binding. Mutations of the *fzp-2*, *fzp-3*, *fzp-7* and *fzp-8* alleles are shown. BD1, maize BRANCHED SILKLESS; BD1B, duplicate of BD1; LEP, *Arabidopsis* LEAFY PETIOLE; *Arabidopsis* ESR1, ENHANCER OF SHOOT REGENERATION1; TINY, *Arabidopsis* TINY. (C) Transactivation of the GAL4-LUC reporter gene by FZP. Schematics of the constructs used are indicated on the left and described in the Material and Methods section. Relative luciferase activities in *Arabidopsis* leaves that had been co-bombarded with reporter and effector plasmids are indicated on the right. All luciferase activities were expressed in arbitrary units relative to values obtained with the reporter construct alone (None; set arbitrarily at 1). The values shown are averages of results from three independent experiments. Error bars indicate standard deviation.

Ac elements with the *fzp* phenotype (Fig. 5B), the region flanking these elements was isolated and sequenced. Both *Ac* elements were inserted on the region of chromosome 7 corresponding to the AP004570 PAC clone approximately 3 kb apart from each other (Fig. 5A). No genes were predicted around the proximal *Ac* element, however, the distal *Ac* element was inserted in an ORF encoding a putative protein containing a sequence similar to the ethylene-responsive element-binding factor (ERF) domain. Alterations in this ORF were found in the other four *fzp* alleles and also in *fzp-FM44*, *fzp-KH56* and *fzp-KH1*, which were then redesignated as *fzp-6*, *fzp-7* and *fzp-8*, respectively (Fig. 6A, Table 1). The sum of the results obtained from the map-based analysis, the transposon tagging and the finding of alterations in all *fzp* lines, led us to conclude that this ERF domain gene indeed represents the *FZP* gene.

The *FZP* gene is a single copy gene, as revealed by homology searches in the rice genomic database, and it encodes a putative protein of 318 amino acids, sharing the highest homology with the maize BD1 protein and its duplicate BD1B. Indeed, *FZP* was found to be identical to the rice ortholog of *BD1* which was recently reported by Chuck et al. (Chuck et al., 2002) (G. Chuck personal communication). FZP and BD1 have completely identical ERF domains (Fig. 6B) and share 59% overall amino acid identity. Other motifs besides the ERF domain that are conserved in FZP and BD1 are shown in Fig. 6A. The region between amino acids 27 and 42 of the FZP protein is Ser-Pro rich and shows significant similarity to PEST sequences, which serve as signals for rapid proteolytic degradation (Rechsteiner and Rogers, 1996). Also consistent with the function of FZP as a transcription factor, a putative bipartite nuclear localization signal is found between amino acids 49 and 66. The C-terminal end is highly conserved in FZP, BD1 and putative orthologs of BD1 from other grass species (G. Chuck and E. Kellogg, personal communication). An acidic region is present within this region, amino acids 246-268 in FZP, and may function as an activation domain.

The ERF domain of FZP is composed of 58 amino acids and is localized close to the N terminus of the protein. From the length and position of the ERF domain within the amino acid sequence, FZP was classified as a class II ERF protein (Fujimoto et al., 2000). The ERF domain of FZP showed high sequence similarity to the domains of other class II ERFs, such as the *Arabidopsis* LEAFY PETIOLE (LEP) (van der Graaff, 2000) and ENHANCER OF SHOOT REGENERATION1 (ESR1) (Banno et al., 2001), with which FZP shares 90% and 72% identity, respectively (Fig. 6B). However, no significant homology was found outside the ERF domain. No other genes with significant overall identity to *FZP* were found in homology searches of the public databases, but the cloning of *FZP*/*BD1*-like genes from other grass species has been reported (Chuck et al., 2002).

The ERF domain and the acidic domain are essential for proper FZP function

ERF transcription factors were first isolated as proteins that bound to the cis-acting motif known as the GCC-box found in the promoters of defense genes, the expression of which is

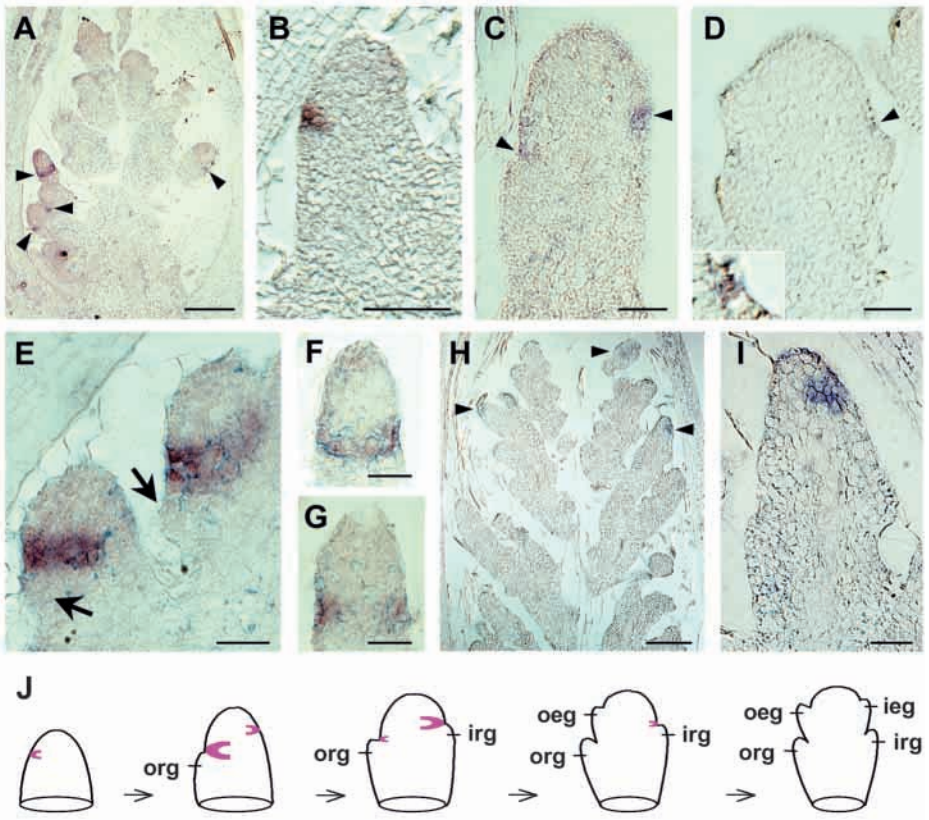

Fig. 7. In situ hybridizations depicting the pattern of *FZP* expression (arrowheads) during the development of wild-type (A-G) and *fzp-2* (H,I) spikelets. (A) Wild-type SAM at the spikelet differentiation stage. *FZP* RNA (arrowheads) is detected in spikelet meristems before and during the formation of rudimentary glume (RG) primordia. (B) Early stage of spikelet meristem (SM) differentiation. *FZP* is expressed just above the position where the RG primordium emerges. (C) SM at early inner RG differentiation stage. While the expression of *FZP* decreases at the outer RG axil, it increases on the iRG side. (D) SM at early palea differentiation stage. *FZP* expression at the inner RG axil persists weakly until the initiation of the palea primordium. Note that *FZP* is not expressed at the position of the lemma and palea primordia initiation or in their axils. (Inset) Higher magnification of the region expressing *FZP*. (E-G) *FZP* expression extends to a half-ring domain. (E) Lateral view. *FZP* expression is interrupted around the circumference of the SM. RG primordia (arrows) emerge right under the domain of *FZP* expression. (F,G) Frontal view of successive transverse sections. *FZP* is expressed at the sides but not at the center of the SM. (H) Late *fzp-2* SAM. *FZP* is expressed at the tip of secondary branches. (I) Higher magnification of the tip of a secondary branch. *FZP* is expressed at the axil of a differentiating RG primordium. (J) Schematic representation of the spatial and temporal expression of *FZP* during the differentiation of a spikelet. org, outer rudimentary glume; irg, inner rudimentary glume; oeg, outer empty glume; ieg, inner empty glume. Scale bars: 100 μm.

induced by ethylene (Sessa et al., 1995; Ohme-Takagi and Shinshi, 1995). The *fzp-2* and *fzp-7* mutations caused an alteration of one of six conserved amino acids of the ERF domain that are thought to confer GCC box-specific binding (Allen et al., 1998; Hao et al., 1998) and resulted in severe *fzp* phenotypes (Fig. 6, Table 1). Alteration of a conserved amino acid of the ERF domain not required for specific GCC-box binding in *fzp-3*, however, resulted in the weak *fzp* phenotype, suggesting that the FZP transcription factor may also regulate its target(s) by GCC box-mediated gene expression.

Three other alleles had mutations in the conserved C-terminal region (Fig. 6A). In *fzp-4* and *fzp-1*, the insertion of an *Ac* element and a *Houba* copia-type retroelement (Panaud et al., 2002) caused the formation of putative premature stop codons upstream and at the beginning of the acidic domain, respectively, and resulted in severe phenotypes (Table 1). In *fzp-6*, an insertion of a putative copia-like retrotransposon caused the formation of a stop codon at the end of the acidic domain, leading to the temperature-sensitive phenotype. The formation of premature stop codons before the acidic region in *fzp-1* and *fzp-4* might have resulted in the formation of proteins lacking transcriptional activation activity, leading to the severe phenotypes observed. Although the molecular basis of the temperature-sensitive phenotype of *fzp-6* is unknown, the fact that three *fzp* alleles had mutations at the C terminus strongly indicate that this conserved region must also be necessary for proper FZP function in addition to the ERF domain.

In addition, two more alleles produced the severe *fzp* phenotype. In *fzp-8*, a single nucleotide base change resulted in the formation of a premature stop codon at the end of the ERF domain that might result in a non-functional product. In *fzp-5*, no mutation was detected within the *FZP* sequence, but an insertion of *Karma*, a LINE-type retroelement (Komatsu et al., 2003), was found approx. 2.5 kb upstream of the *FZP* gene at a site that is 9 bp distant from the insertion point of the second cosegregating *Ac* element of *fzp-4*. As a severe phenotype is observed for *fzp-5*, this region might be a cis-acting element of *FZP* and, in this case, may also account for the severe phenotype observed for *fzp-4* alleles. Alternatively, as transposon activity has been associated with epimutations found in a variety of organisms from plants to mammals (reviewed by Martienssen and Colot, 2001; Whitelaw and Martin, 2001), we cannot rule out the possibility that the insertion of *Karma* causes the epigenetic effects in *fzp-5*.

FZP functions as a transcriptional activator

The ability of FZP to regulate transcription in plant cells was tested by using transient assays (Fig. 6C). A luciferase (LUC)-encoding reporter gene, GAL4-LUC, which contains five copies of the yeast GAL4-binding site fused to LUC, and an effector plasmid, GAL4DB-FZP, consisting of the coding region of *FZP* fused to the GAL4 DNA-binding domain under the control of the cauliflower mosaic virus (CaMV) 35S promoter (Fig. 6C left) were delivered to *Arabidopsis* leaves by particle bombardment. LUC activity increased 16.6-fold when the reporter plasmid was co-expressed with the *FZP*

effector plasmid (Fig. 6C right). The GAL4 DNA-binding domain alone (GAL4DB) also increased LUC activity 4.7-fold. Nevertheless, the increase in LUC activity induced by GAL4DB-FZP was 3.5 times higher than the one induced by GAL4DB, and indicates that FZP functions as a transcriptional activator.

FZP is expressed at the axils of rudimentary glumes primordia

The temporal and spatial expression of *FZP* was determined by in situ hybridization analyses. *FZP* expression was restricted to a very short period during the development of inflorescences (Fig. 7). *FZP* RNA was first detected at the early stage of spikelet meristem (SM) development, when the primordium of the outer rudimentary glume is starting to become apparent (Fig. 7A,B). The examination of several consecutive sections revealed that *FZP* expression extended to a half-ring domain, at the base of which the rudimentary glume (RG) primordium developed (Fig. 6E-G). While the expression level in the outer RG axil decreased, expression at the opposite side of the SM, where the inner RG develops, increased (Fig. 7C). *FZP* expression in the axil of the inner RG could be detected until the time the outer empty glume primordium began to form (Fig. 7D). It should be noted that no axillary meristem formation was observed in the axils of rudimentary glume primordia in wild-type spikelets. No signal was observed for sense probe controls (data not shown). A scheme representing the pattern of *FZP* expression is shown in Fig. 7J. The expression pattern of the *FZP* gene was very similar to the one observed for *BD1*, whose transcripts were detected in a semicircular domain above the developing glumes, and it strongly supports our proposal that rudimentary glumes are the actual counterparts of the glumes of other grass species.

The mutations in the *fzp-2* and *fzp-7* alleles were caused by single amino acid changes at the ERF domain. Expecting that *FZP* transcripts could be produced in these mutants, we analyzed their expression pattern using in situ hybridization (Fig. 7H,I). A similar pattern observed for wild-type was detected in *fzp-2* and *fzp-7*. *FZP* expression was restricted to the time of formation of the rudimentary glume-like structures. *FZP* was not expressed in developing ectopic axillary meristems and transcripts were observed only in the apical part of secondary branches where new rudimentary glume primordia were being formed. This pattern of expression supports our observation that rudimentary glumes are repeatedly produced in *fzp* mutants.

DISCUSSION

Rudimentary glumes are actually glumes

The spikelet is a structure unique to grasses and is present in all grass species. The structure of the rice spikelet in particular has been a matter of discussion for a long time. The most accepted interpretation dictates that the pair of empty glumes together with the floret compose a spikelet, and rudimentary glumes are regarded as bracts surrounding it (Hoshikawa, 1989; Bell, 1991; Takeoka et al., 1993). An alternative view proposes that the two empty glumes are sterile equivalents of lemmas and that the rudimentary glumes correspond to glumes as known in other grass species (reviewed by Takeoka et al., 1993). We determined that the expression domain of *FZP* during the development of rice inflorescences was localized in the axils of rudimentary glume primordia of spikelet meristems, and that floral meristems were replaced by higher order branches composed of several rudimentary glumes in *fzp* mutant alleles. Similarly, the transcripts of the ortholog in maize, *BD1*, were found in a narrow region between the spikelet meristem and the glumes (Chuck et al., 2002), and *bd1* spikelet meristems could not switch to floral meristem production, instead continuing to form glumes and spikelet-like meristems (Colombo et al., 1998). By comparison, we propose that the rudimentary glumes of rice are the equivalents of glumes of other grass species and, consequently, the empty glumes correspond to sterile lemmas and subtending florets might have been lost during the course of evolution as suggested by Arber (Arber, 1934).

FZP maintains floral fate

The phyllotaxy of ectopic branch meristem formation and the generation of ectopic rudimentary glumes indicated that the meristems formed in the inflorescence of *fzp* mutants had acquired spikelet meristem (SM) identity. In addition, the phenotype caused by the weak alleles indicated that these SMs had the capacity to form floral organs if they acquired floral meristem identity. In the wild-type inflorescence, the SM proceeds to the generation of empty glumes without forming axillary meristems from rudimentary glumes. In contrast, the defect of *fzp* mutants was the generation of meristems in the axils of rudimentary glumes. By integrating the information above, it is possible to explain the function of FZP in two ways (Fig. 8). First, the primary function of FZP is the suppression of shoot branching within the spikelet (Model 1). Second, FZP is a positive regulator of floral meristem identity (Model 2). We showed that *FZP* is expressed in a half-ring pattern in a region immediately above where rudimentary glumes are formed, which also coincides with the region where axillary meristems are generated in *fzp* mutants. From this data we favor the first interpretation that FZP inhibits axillary meristem formation, but the second possibility cannot be ruled out. In

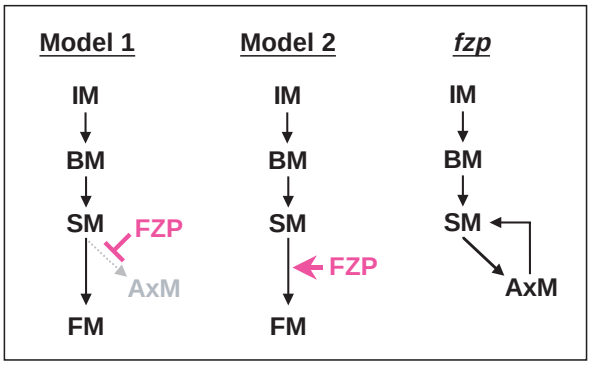

Fig. 8. Models representing the function of FZP during the development of rice spikelets. In wild-type plants, the inflorescence meristem (IM) generates branch meristems (BM) that in turn generate spikelet meristems (SM). Model 1, FZP acts to repress the formation of axillary meristems (AxM) from the SM and ensure that the SM acquires floral meristem (FM) identity. Model 2, FZP induces the transition from SM to FM identity. In *fzp* mutants, the transition to FM identity does not take place and ectopic AxMs behave as SMs.

both cases, the transition from spikelet to floral identity is prevented in *fzp* mutants and ectopic axillary meristems behave as SMs generating rudimentary glumes with axillary meristems that reiterate the same process.

FZP acts as a transcriptional activator by GCC-box binding

The ERF proteins are plant-specific transcription factors that were originally identified as ethylene-responsive element binding proteins (Sessa et al., 1995; Ohme-Takagi and Shinshi, 1995). In addition to their roles during stress responses, some ERF genes, such as *TINY*, *LEP* and *ESR1*, have been implicated to participate in plant development because overexpression of these genes affected normal growth (Wilson et al., 1996; van der Graaff et al., 2000; Banno et al., 2001; Kirch et al., 2003). However, their actual roles in plant development have not yet been clarified because of the lack of loss-of-function mutants. It has been evaluated that 124 ERF-like proteins are encoded by the *Arabidopsis* genome (Riechmann et al., 2000). Based on amino acid identities within the ERF domain, ERFs can be grouped into 3 classes (Fujimoto et al., 2000) and according to this classification *FZP* is a member of class II. Interestingly, transient assays of two class II ERFs of *Arabidopsis* revealed that both had transcriptional repressor activity (Fujimoto et al., 2000) and a repression domain was found to be conserved in most, but not all, of class II ERFs, although the precise molecular basis of its action is still unknown (Ohta et al., 2001). *FZP*, however, lacks this repression domain and is not likely to work as a transcriptional repressor. Consistent with this, we have shown that three *fzp* alleles have mutations at a putative activation domain. Furthermore, transient assays have shown that *FZP* acts as a transcriptional activator. Therefore, although *fzp* mutant phenotypes indicate that *FZP* functions to suppress axillary meristem formation, it probably activates the transcription of downstream genes that are involved in the suppression of branching.

The ERF domain exhibits a novel mode of DNA recognition by a β-sheet structure. NMR analyses revealed that the majority of the conserved residues in ERF sequences are necessary for either the stabilization of the protein structure or DNA recognition. Six of these residues have both attributes and are responsible for the specific recognition of the GCC-box by the ERF domain. It has been proposed that alteration of these residues could cause truncation in the binding geometry, affecting specificity (Allen et al., 1998; Hao et al., 1998). Among the eight *fzp* alleles examined in this study, three showed an amino acid exchange within the ERF domain. Substitution of one of these six residues caused severe phenotypes in *fzp-2* and *fzp-7*. In contrast, in the weak *fzp-3* allele substitution of an amino acid that was shown to confer only structural stability by NMR analysis was found. Our data is therefore consistent with the results obtained from in vitro analyses of GCC-box mediated DNA-protein interaction. Although the features of ERF proteins as transcription factors are well studied in vitro, their actual in vivo functions are less understood owing to the lack of loss-of-function mutants. So far, *Arabidopsis ABI4* and the maize *BD1* are the only ERF family genes for which loss-of-function mutants are reported (Finkelstein et al., 1998; Chuck et al., 2002). The identification of a series of *fzp* mutant alleles will therefore be useful for further studies on the molecular function of ERF transcription factors in plant development.

A conserved mechanism of inflorescence formation unique to grasses

We have determined that the phenotype of *fzp* mutants is analogous to the phenotype of *bd1* mutants. Similarly, the expression patterns and the predicted functions of *FZP* and *BD1* are extremely similar. The conservation of function of two ERF transcription factors, whose expression is specific to spikelet meristems and whose sequence is conserved in other grass species but is not found in the model dicot specie *Arabidopsis*, indicates that an additional level of genetic regulation is required for the formation of inflorescences in grasses. The identification of other genes acting upstream or downstream in this regulatory pathway is expected to clarify the genetic framework that directs the transition from branch to spikelet and spikelet to floret meristems, and possibly the integration with the already known genes that regulates the formation of floret organs (McSteen et al., 2000; Goto et al., 2001).

We thank Dr M. Maekawa for the *fzp-2* allele; Dr E. Amano for the *fzp-3*, *fzp-7* and *fzp-8* alleles; Dr M. Ohme-Takagi and Dr K. Hiratsu for the reporter and effector constructs and assistance during the transient assays; Dr G. Chuck and Dr E. Kellogg for sharing valuable information on the maize *BD1* gene and its grass orthologs, and Y. Satake for technical assistance at the mapping stage. M.K. was supported by a JSPS research fellowship for young scientists.

REFERENCES

Allen, M. D., Yamasaki, K., Ohme-Takagi, M., Tateno, M. and Suzuki, M. (1998). A novel mode of DNA recognition by a beta-sheet revealed by the solution structure of the GCC-box binding domain in complex with DNA. *EMBO J.* **17**, 5484-5496.

Ambrose, B. A., Lerner, D. R., Ciceri, P., Padilla, C. M., Yanofski, M. F. and Schmidt, R. (2000). Molecular and genetic analysis of the *silky1* gene reveal conservation in floral organ specification between eudicots and monocots. *Mol. Cell* **5**, 569-579.

Arber, A. (1934). *The gramineae: A study of cereal, bamboo, and grass.* Cambridge, UK: Cambridge University Press.

Banno, H., Ikeda, Y., Niu, Q. W. and Chua, N. H. (2001). Overexpression of *Arabidopsis ESR1* induces initiation of shoot regeneration. *Plant Cell* **13**, 2609-2618.

Battey, N. H. and Tooke, F. (2002). Molecular control and variation in the floral transition. *Curr. Opin. Plant Biol.* **5**, 62-68.

Bell, A. D. (1991). *Plant Form: An Illustrated Guide to Flowering Plant Morphology.* New York: Oxford University Press.

Chuck, G., Muszynski, M., Kellogg, E., Hake, S. and Schmidt, R. J. (2002). The control of spikelet meristem identity by the *branched silkless1* gene in maize. *Science* **298**, 1238-1241.

Coen, E. S. and Nugent, J. M. (1994). Evolution of flowers and inflorescences. *Development Suppl.* 107-116.

Colombo, L., Marziani, G., Masiero, S., Wittich, P. E., Schmidt, R. J., Gorla, M. S. and Pe, M. E. (1998). *BRANCHED SILKLESS* mediates the transition from spikelet to floral meristem during *Zea mays* ear development. *Plant J.* **16**, 355-363.

Enoki, H., Izawa, T., Kawahara, M., Komatsu, M., Koh, S., Kuozuka, J. and Shimamoto, K. (1999). *Ac* as a tool fot the functional genomics of rice. *Plant J.* **19**, 605-614.

Fedoroff, N. V., Wessler, S. and Shure, M. (1983). Isolation of the transposable maize controlling elements *Ac* and *Ds*. *Cell* **35**, 235-242.

Finkelstein, R. R., Wang, M. L., Lynch, T. J., Rao, S. and Goodman, H. M. (1998). The *Arabidopsis* abscisic acid response locus *ABI4* encodes an APETALA2 domain protein. *Plant Cell* **10**, 1043-1054.

Fujimoto, S. Y., Ohta, M., Usui, A., Shinshi, H. and Ohme-Takagi, M.

(2000). *Arabidopsis* ethylene-responsive element binding factors act as transcriptional activators or repressors of GCC box-mediated gene expression. *Plant Cell* **12**, 393-404.

Goto, K., Kyozuka, J. and Bowman, J. L. (2001). Turning floral organs into leaves, leaves into floral organs. *Curr. Opin. Genet. Dev.* **11**, 449-456.

Hao, D., Ohme-Takagi, M. and Sarai, A. (1998). Unique mode of GCC box recognition by the DNA-binding domain of ethylene-responsive element-binding factor (ERF domain) in plant. *J. Biol. Chem.* **273**, 26857-26861.

Hoshikawa, K. (1989). *The Growing Rice Plant.* Tokyo: Nobunkyo.

Izawa, T., Ohnishi, T., Nakano, T., Ishida, N., Enoki, H., Hashimoto, H., Itoh, K., Terada, R., Wu, C., Miyazaki, C. et al. (1997). Transposon tagging in rice. *Plant Mol. Biol.* **35**, 219-229.

Kang, H. G., Jeong, J. S., Lee, S. and An, G. (1998). Identification of class B and class C floral organ identity genes from rice plants. *Plant Mol. Biol.* **38**, 1021-1029.

Kinoshita, T. and Takahashi, M. (1991). The one hundredth report of genetical studies on a rice plant. *J. Faculty Agric. Hokkaido Univ.* **65**, 1-61.

Kirch, T., Simon, R., Grunewald, M. and Werr, W. (2003). The *DORNROSCHEN/ENHANCER OF SHOOT REGENERATION1* gene of *Arabidopsis* acts in the control of meristem cell fate and lateral organ development. *Plant Cell* **15**, 694-705.

Komatsu, M., Maekawa, M., Shimamoto, K. and Kyozuka, J. (2001). The *LAX1* and *FRIZZY PANICLE 2* genes determine the inflorescence architecture of rice by controlling rachis-branch and spikelet development. *Dev. Biol.* **231**, 364-373.

Komatsu, M., Shimamoto, K. and Kyozuka, J. (2003). Two-step regulation and continuous retrotransposition of the rice LINE-type retrotransposon *Karma*. *Plant Cell* (in press).

Kyozuka, J. (1999). Flower development of rice. In *Molecular Biology of Rice* (ed. K. Shimamoto), pp. 43-58. Tokyo: Springer-Verlag.

Kyozuka, J., Kobayashi, T., Morita, M. and Shimamoto, K. (2000) Spatially and temporally regulated expression of rice MADS box genes with similarities to *Arabidopsis* class A, B and C genes. *Plant Cell Physiol.* **41**, 710-718.

Mackill, D. J., Pinson, S. R. M. and Rutger, J. N. (1991). *Frizzy panicle*, an EMS-induced mutant in the Japonica cultivar M-201. *Rice Genet. Newsl.* **9**, 100-102.

Martienssen, R. A. and Colot, V. (2001). DNA methylation and epigenetic inheritance in plants and filamentous fungi. *Science* **293**, 1070-1074.

McSteen, P., Laudencia-Chingcuanco, D. and Colasanti, J. (2000). A floret by any other name: control of meristem identity in maize. *Trends Plant Sci.* **5**, 61-66.

Michaels, S. D. and Amasino, R. M. (1998). A robust method for detecting single-nucleotide changes as polymorphic markers by PCR. *Plant J.* **14**, 381-385.

Murai, M. and Iizawa, M. (1994). Effects of major genes controlling morphology of panicle in rice. *Breed. Sci.* **44**, 247-255.

Ohme-Takagi, M. and Shinshi, H. (1995). Ethylene-inducible DNA binding proteins that interact with an ethylene-responsive element. *Plant Cell* **7**, 173-182.

Ohta, M., Ohme-Takagi, M. and Shinshi, H. (2000). Three ethylene-responsive transcription factors in tobacco with distinct transactivation functions. *Plant J.* **22**, 29-38.

Ohta, M., Matsui, K., Hiratsu, K., Shinshi, H. and Ohme-Takagi, M. (2001). Repression domains of class II ERF transcriptional repressors share an essential motif for active repression. *Plant Cell* **13**, 1959-1968.

Panaud, O., Vitte, C., Hivert, J., Muzlak, S., Talag, J., Brar, D. and Sarr, A. (2002). Characterization of transposable elements in the genome of rice (*Oryza sativa* L.) using Representational Difference Analysis (RDA). *Mol. Genet. Genomics* **268**, 113-121.

Rechsteiner, M. and Rogers, S. W. (1996). PEST sequences and regulation by proteolysis. *Trends Biochem. Sci.* **21**, 267-271.

Riechmann, J. L., Heard, J., Martin, G., Reuber, L., Jiang, C., Keddie, J., Adam, L., Pineda, O., Ratcliffe, O. J., Samaha, R. R. et al. (2000). *Arabidopsis* transcription factors: genome-wide comparative analysis among eukaryotes. *Science* **290**, 2105-2110.

Sessa, G., Meller, Y. and Fluhr, R. (1995). A GCC element and a G-box motif participate in ethylene-induced expression of the PRB-1b gene. *Plant Mol. Biol.* **28**, 145-153.

Takeoka, Y., Mamaum, A. A., Wada, T. and Kaufman, P. B. (1992). *Reproductive Adaptation of Rice to Environmental Stress.* Tokyo: Japan Scientific Society Press.

Takeoka, Y., Shimizu, M. and Wada, T. (1993). Panicles. In *Science of the Rice Plant*, vol. I (ed. T. M. a. H. Hoshikawa), pp. 295-326. Tokyo: Nobunkyo.

Trigrlia, T., Peterson, M. G. and Kemp, D. J. (1988). A procedure for in vitro amplification of DNA segments that lie outside the boundaries of known sequences. *Nucl. Acids Res.* **19**, 8186.

van der Graaff, E., Dulk-Ras, A. D., Hooykaas, P. J. and Keller, B. (2000). Activation tagging of the *LEAFY PETIOLE* gene affects leaf petiole development in *Arabidopsis thaliana*. *Development* **127**, 4971-4980.

Whitelaw, E. and Martin, D. I. (2001). Retrotransposons as epigenetic mediators of phenotypic variation in mammals. *Nat. Genet.* **27**, 361-365.

Wilson, K., Long, D., Swinburne, J. and Coupland, G. (1996). A *Dissociation* insertion causes a semidominant mutation that increases expression of *TINY*, an *Arabidopsis* gene related to *APETALA2*. *Plant Cell* **8**, 659-671.